CHIN. PHYS. LETT. Vol. 32, No. 6 (2015) 063302

Generation of Isolated Attosecond Pulse from Asymmetric Molecular Ions by Introducing Half-Cycle-Like Laser Fields *

LIU Sha-Sha(刘莎莎), MIAO Xiang-Yang(苗向阳)**

College of Physics and Information Engineering, Shanxi Normal University, Linfen 041004

(Received 26 February 2015)

We propose an efficient method for the generation of an isolated attosecond pulse from the asymmetric molecular ions HeH^{2+} by adding a half-cycle-like field (HCLF) to the fundamental driving laser field. The high-order harmonic generation (HHG) is investigated by numerically solving the time-dependent Schrödinger equation. By performing the time-frequency distributions and the electronic wave packet probability densities, we find that the optimizing combined field is not only useful for extending the HHG cutoff, but also for simplifying the recombination channels through controlling the electron localization. In addition, by adjusting the intensity of the HCLF, a dominant short quantum path is selected to contribute the HHG spectrum. As a result, a 75-as isolated attosecond pulse is obtained by superposing a proper range of the harmonics.

PACS: 33.80.Rv, 31.30.Gs, 42.50.Hz DOI: 10.1088/0256-307X/32/6/063302

A great deal of attention has been paid to the dynamics of atoms or molecules exposed to an intense ultrashort laser field,[1−5] which produced many highly nonlinear-nonperturbative phenomena, such as the above threshold ionization,[6] Coulomb explosion,[7] and the high-order harmonic generation (HHG).[4,5] Among them the HHG is well known due to its important applications in generating isolated attosecond pulses.[8] The HHG can be well understood by a semiclassical three-step model[9] consisting of ionization, acceleration and recombination. Based on this model, the HHG can be efficiently controlled by modulating different steps of the harmonic processes to produce an ultrabroad supercontinuum. Currently, several schemes have been proposed to generate an isolated attosecond pulse, such as few-cycle laser driving,[10] polarization gating,[11] double optical gating[12] and a multi-color scheme.[13,14] Compared with the HHG from atoms, HHG from molecules is more complex due to the additional degree of molecular structure. However, it also provides an additional parameter to control the electron motion and the attosecond pulse generation. For the symmetric two-center molecule, Zuo *et al.*[15] and Moreno *et al.*[16] found that both the harmonic intensity and the cutoff energy of the harmonic spectrum from H_2^+ at a higher initial excited vibrational state are enhanced. Lein[4] theoretically proved that the harmonic spectra are sensitive to the laser-induced vibrational motion. Taking advantage of the alignment dependence of HHG in N_2 molecules, Yao *et al.*[17] theoretically realized the selection of a single quantum path by constructing a driving laser field with a rapidly varying waveform. Recently, the HHG from the simplest asymmetric molecular ion HeH^{2+} has been widely investigated. Bian *et al.*[18] showed that the laser-induced electron transfer plays an important role in the multichannel harmonic generation from HeH^{2+}. Miao *et al.*[19,20] discussed the physical image in harmonic emission and the distinguishing of recombination channels from HeH^{2+} in detail.

In this Letter, the harmonic spectra from HeH^{2+} driven by the monochromatic laser field with different peak intensities are firstly investigated. Based on the numerical results and previous work,[19] the recombination channels are simplified and the harmonic spectrum with less modulation in the plateau is obtained for the case of a low laser intensity. However at the same time, the cutoff energy is also reduced with the decrease of the laser intensity. Then we propose a possible scheme to produce isolated attosecond pulses from HeH^{2+} exposed to a combined field of a fundamental laser with a low peak intensity and a half-cycle-like field (HCLF) with a proper peak intensity. The HCLF is a highly asymmetric pulse, which contains a strong and sharp peak followed by a long and weak tail. Since a terahertz half-cycle pulse (HCP) has been generated experimentally,[21] it provides an opportunity for generating half-cycle pulses with other frequency regimes. The HCLF has been used widely in many studies due to its asymmetric field.[22−24] Most recently, a new scheme was proposed by Zhang *et al.*[25] to produce super-bright attosecond pulses via the superposition of few-cycle and half-cycle pulses with an optimized delay time or laser wavelengths and intensity matching. The advantage of the HCLF is that the effect of the pulse tail in the ionization pro-

*Supported by the National Natural Science Foundation of China under Grant No 11404204, the Key Project of the Ministry of Education of China under Grant No 211025, the Research Fund for the Doctoral Program of Higher Education of China under Grant No 20111404120004, and the Natural Science Foundation for Young Scientists of Shanxi Province under Grant No 2009021005.

**Corresponding author. Email: sxxymiao@126.com

© 2015 Chinese Physical Society and IOP Publishing Ltd

cess can be neglected. As it acts like an impulsive kick, the ionized electrons can gain higher kinetic energy in the next accelerating process. In this work, a 75-as isolated attosecond pulse can be obtained theoretically by superposing harmonics generated from the optimizing combined field.

The HHG from HeH^{2+} can be studied by numerically solving the time-dependent Schrödinger equation (TDSE) via the standard second-order split operator method[26,27] and the parallel quantum wave-packet computer code LZH-DICP.[28,29] The TDSE can be written as ($e = m_e = \hbar = 1$)

$$i\frac{\partial}{\partial t}\psi(R,z,t) = [H_0 + V(t)]\psi(R,z,t), \tag{1}$$

where R is the relative nuclear coordinate, z is the electronic coordinate measured with respect to the center-of-mass of the two nuclei, and $V(t)$ is the electron potential including the laser-molecule interaction. The field-free Hamiltonian has an ordinary form

$$H_0 = T_n + T_e + V(z,R), \tag{2}$$

where $T_n = -\frac{1}{2\mu}\frac{\partial^2}{\partial R^2}$ and $T_e = -\frac{1}{2\mu_e}\frac{\partial^2}{\partial z^2}$ denote the nuclear and the electronic kinetic-energy operator, respectively, with $\mu = (1/m_H + 1/m_{He})^{-1}$ and $\mu_e = (m_H + m_{He})/(m_H + m_{He} + 1)$ being the reduced masses. Here m_H and m_{He} are the masses of H and He, respectively. The Coulomb potential $V(z,R)$ can be written as

$$V(z,R) = \frac{C_H C_{He}}{R+a} - \frac{C_H}{\sqrt{(z-z_H)^2+b}} - \frac{C_{He}}{\sqrt{(z-z_{He})^2+b}}, \tag{3}$$

where C_H and C_{He} are the electron charges of the nuclei, and $z_H = m_{He}/(m_H + m_{He})R$ and $z_{He} = -m_H/(m_H + m_{He})R$ are the positions of H and He, respectively. The soft-core parameters $a = 0.01$ and $b = 0.3$ have been chosen, thus the model of HeH^{2+} corresponds to the $2p\sigma$ bound state energy and equilibrium distance of -0.5317 and 3.9 a.u.,[30] respectively.

The interaction between the laser field and molecules is treated in the dipole approximation and length gauge[31]

$$V(t) = \Big[\frac{C_{He}m_H - C_H m_{He}}{m_H + m_{He}}R + \Big(1 + \frac{C_H + C_{He} - 1}{m_H + m_{He} + 1}\Big)z\Big] \times E(t). \tag{4}$$

The combined field can be expressed as

$$E(t) = E_1 f_1(t)\cos(\omega t) + E_2 f_2(t - t_{delay}) \cdot \cos[\omega(t - t_{delay}) - \phi], \tag{5}$$

where E_1 and E_2 are the peak values of the fundamental driving and the manipulating electric field strength, respectively. The frequency $\omega = 0.038$ a.u. corresponds to the wavelength 1200 nm for the two pulses. The fundamental pulse envelope $f_1(t)$ is a three-optical-cycle trapezoidal envelope with one cycle ramp on, one cycle constant, and one cycle ramp off. The manipulating pulse envelope $f_2(t)$ is a Gaussian envelope, which can be expressed as $f_2(t) = \exp[-4\ln(2)(t - t_{delay})^2/\tau^2]$, where $T_L = 2\pi/\omega$ is the optical cycle (o.c.) corresponding to the wavelength 1200 nm (1 o.c.=4 fs), and τ is the temporal full width at half maximum of the manipulating pulse. In this work, we choose $\tau = 0.4T_L$ to ensure that the manipulating pulse acts as a half-cycle-like field (HCLF). The relative time delay t_{delay} and relative phase between the two pulses are set to be $1.5T_L$ and π.

According to the Ehrenfest theorem,[32] the time-dependent dipole acceleration can be written as

$$d_A(t) = \langle\psi(R,z,t)|-\frac{\partial V_C}{\partial z} + \Big(1 + \frac{C_H + C_{He} - 1}{m_H + m_{He} + 1}\Big)E(t)|\psi(R,z,t)\rangle. \tag{6}$$

To collect detailed information about the harmonic emission from HeH^{2+}, the harmonic spectrum and the time-frequency distribution are calculated by means of Fourier transformation and wavelet transformation, respectively.[20]

Finally, an attosecond pulse can be generated by superposing several harmonics

$$I(t) = \Big|\sum_q \Big(\int_0^t d_A(t)e^{-iq\omega t}dt\Big)e^{iq\omega t}\Big|^2. \tag{7}$$

The ground state of HeH^{2+} is a repulsive state,[33] thus photodissociation and HHG will happen simultaneously under the effect of a strong laser field. In this work, the first excited state ($2p\sigma$) of HeH^{2+} which is a bound state is chosen to be the initial state to investigate the HHG process rather than the photodissociation process. In Figs. 1(a) and 1(b), we show the high-order harmonic spectra for the HeH^{2+} molecule ion driven by the fundamental laser pulse with peak intensities $I_1 = 7\times10^{14}$ W/cm^2 and $I_1 = 1\times10^{14}$ W/cm^2, respectively. At first glance, the harmonic spectra share the following common features: they drastically decay for the first few-order harmonics, followed by a plateau region; finally they cut off in the high-order region. However, there are some distinct differences between them, especially in the plateau region. For the higher laser intensity, the plateau region is accompanied with obvious modulations and we can find three clear minima at the high-energy part. This spectrum is disadvantageous to obtain an isolated attosecond pulse by superposing the harmonics in the plateau region. When the laser intensity is reduced to

1×10^{14} W/cm^2, we can see that the modulation of the harmonic spectrum in the plateau region from 75th to 200th is weaker than the case of the higher laser intensity. According to the previous work,[20] we know that the modulation of the harmonic spectrum is closely related to the recombination channels and the electronic wave packet probability densities. In Figs. 1(c) and 1(d), we present the time-dependent electronic wave packet probability densities corresponding to the higher and lower laser intensities. For the higher laser intensity, the electrons are distributed in the region of $z > 0$ and $z < 0$, i.e., the electrons are distributed around the two nuclei. This will result in the occurrence of different recombination channels contributed by the electrons ionized from different nuclei. Here due to the multichannel interference effect in the recombination process, the larger modulations appear on the harmonic spectrum for the higher laser intensity. However, for the lower laser intensity, the electrons are mostly concentrated on one of the nuclei (the region of $z > 0$). For the electrons ionized from the same nucleus, the recombination channels are simpler than the case of the higher laser intensity. Thus when the laser intensity is reduced, the harmonic spectrum in the plateau region becomes smoother with the simplification of the recombination channels. Thus for HeH^{2+}, the laser field with a lower peak intensity is more applicable than the higher laser intensity to obtain an isolated attosecond pulse.

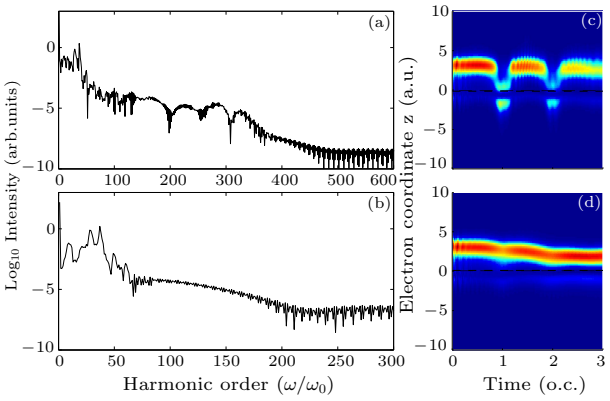


Fig. 1. The harmonic spectra of HeH^{2+} driven by the fundamental laser pulse with peak intensities (a) $I = 7\times10^{14}$ W/cm^2 and (b) $I = 1\times10^{14}$ W/cm^2. Here (c) and (d) are the time-dependent electronic wave packet probability densities corresponding to higher and lower laser intensities in (a) and (b), respectively.

However, when the laser intensity is reduced to 1×10^{14} W/cm^2, the maximum energy that the ionized electrons can gain in the acceleration process is bound to be reduced and the narrow plateau region is also limited to generate an isolated attosecond pulse with short duration. The half-cycle-like field (HCLF), homochromy with the driving laser field, is used to manipulate the accelerating process of the ionized electrons. Through the combined field, the harmonic emission with less modulation and high cutoff energy is expected to be achieved.

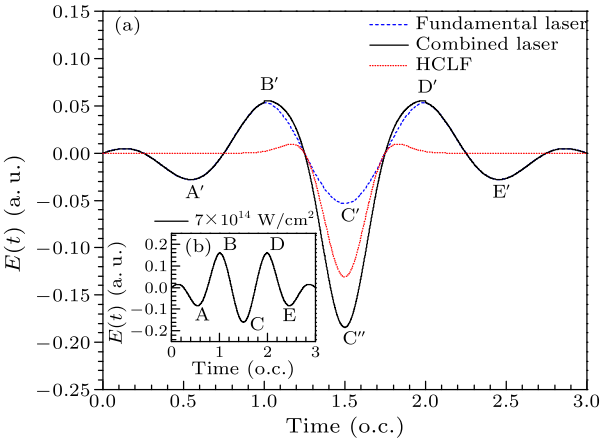


Fig. 2. (a) The black solid line is the profile of the combined field, which is synthesized by the fundamental three-cycle trapezoidal field (blue dashed line) with the peak intensity $I_1 = 1\times10^{14}$ W/cm^2 and the half-cycle-like field (HCLF) (red dotted line) with the peak intensity $I_2 = 6\times10^{14}$ W/cm^2. (b) The profile of the monochromatic driving field with the peak intensity $I = 7\times10^{14}$ W/cm^2.

In Fig. 2(a) we present the 3-cycle fundamental laser field (blue dashed line), the half-cycle-like field (HCLF) (red dotted line) and the combined field (black solid line) of the fundamental field and the HCLF, respectively. To clearly identify the effect of the combined field to the HHG, we choose the fundamental field with a peak intensity of 1.0×10^{14} W/cm^2 and the HCLF with a peak intensity of 6.0×10^{14} W/cm^2 to make sure that the intensity of peak C″ of the combined field is equal to the monochromatic driving field with a peak intensity of 7.0×10^{14} W/cm^2. The profile of the monochromatic driving field with a peak intensity of 7.0×10^{14} W/cm^2 is presented in Fig. 2(b). Seen from this figure, there are five peaks labeled as A, B, C, D and E. According to the three-step model,[9] when the molecular ions are exposed to the monochromatic driving laser, first, the electrons are ionized around the first peak A; secondly, the ionized electrons are accelerated by the following peak B; finally, when the laser field reverses its direction, the accelerated electrons recombine with the parent ions and emit photons between B and C peaks. Thus during the interaction between the laser field and HeH^{2+} molecular ions, there are three major independent HHG processes (ABC, BCD and CDE) contributing to the harmonic generation. When the laser intensity is reduced, the maximum energies of these three processes (A′B′C′, B′C′D′ and C′D′E′) are bound to be decreased and the cut-off energy of the harmonic spectrum will shift to the lower order. For the combined field, the intensity of peak C″ is enhanced due to the introduction of the HCLF. The

maximum energy of the B′C″D′ HHG process will be extended.

To understand the underlying contributions of the recombination channels in HHG, the time-frequency distributions for the monochromatic driving field and the combined field are shown in Figs. 3(a) and 3(b). Laser parameters of the monochromatic driving field and the combined field are the same as the black solid lines in Figs. 2(b) and 2(a). For the monochromatic driving field with a peak intensity of $7.0\times10^{14}\,\mathrm{W/cm^2}$, three major emission events contribute to the high-order region due to the ABC, BCD and CDE HHG processes. However, for the combined field, when the peak intensity of the fundamental field is reduced to $1.0\times10^{14}\,\mathrm{W/cm^2}$, the maximum energies of the two emission events from 1.0 o.c. to 1.5 o.c. and from 2.0 o.c. to 2.5 o.c. are remarkably dropped off due to the intensity decrease of peaks B′ and D′. By adding the HCLF with a peak intensity of $6.0\times10^{14}\,\mathrm{W/cm^2}$ to the fundamental field with a peak intensity of $1.0\times10^{14}\,\mathrm{W/cm^2}$, the maximum energy of the emission event from 1.5 o.c. to 2.0 o.c. is remarkably extended. As a result, only one emission event contributes to the harmonics in the high-order region, which avoids the strong cycle-by-cycle interference effect.

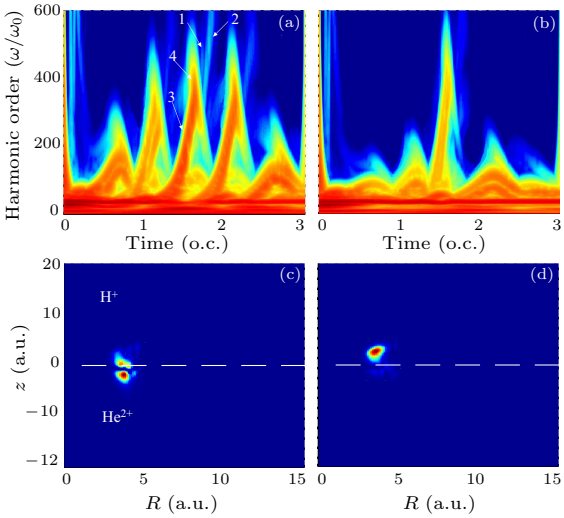


Fig. 3. The time-frequency distributions from the HeH^{2+} in the monochromatic driving field (a) and the combined field (b). Laser parameters for the two cases are the same as the black solid lines in Figs. 2(b) and 2(a). Here (c) and (d) are the electronic wave packet probability densities at $t = 1.0$ o.c. corresponding to the above two cases.

In addition, there are four channels contributing to the emission events from 1.5 o.c. to 2.0 o.c. in Fig. 3(a). According to the discussion in Ref. [20], channels 1, 2, 3 and 4 are corresponding to channels He→e→He, He→e→H, H→e→H and H→e→He, respectively. However, for the combined field, channels 1 (He→e→He) and 2 (He→e→H) in Fig. 3(b) are seriously suppressed. For the emission event from 1.5 o.c. to 2.0 o.c. contributed by the electrons around $t = 1.0$ o.c., we present the electronic wave packet probability densities $P_z(z,t) = \int_0^R dR|\psi(z,R,t)|^2$ at $t = 1.0$ o.c. for the above two cases in Figs. 3(c) and 3(d). For the monochromatic field with the peak intensity $I = 7.0\times10^{14}\,\mathrm{W/cm^2}$, the electrons are distributed around nucleus H^+ and nucleus He^{2+}. While for the combined field, the electrons are mainly distributed in the region of $z > 0$, i.e., around nucleus H^+. Due to the decrease of the electrons concentrated around nucleus He^{2+} at $t = 1.0$ o.c., channels 1 and 2 are obviously suppressed. Thus the multichannel interference is also effectively weakened for the case of the combined field.

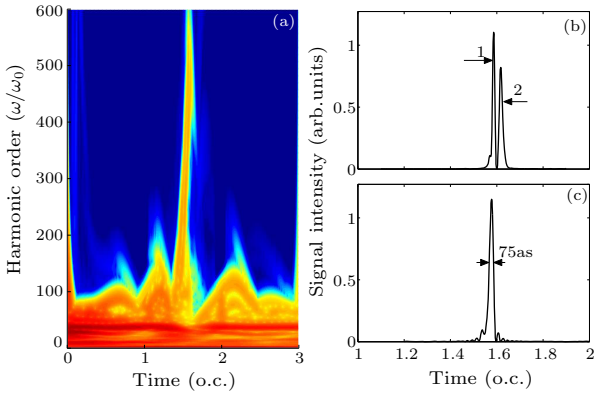


Fig. 4. (a) The time-frequency distribution for the combined field with the peak intensity of the fundamental field $I_1 = 1\times10^{14}\,\mathrm{W/cm^2}$ and the peak intensity of the HCLF $I_2 = 9\times10^{14}\,\mathrm{W/cm^2}$. Here (b) and (c) are the time profiles of the attosecond pulses by superposing harmonics from the 320th to the 450th order for the HCLF with peak intensity $I_2 = 6\times10^{14}\,\mathrm{W/cm^2}$ and $I_2 = 9\times10^{14}\,\mathrm{W/cm^2}$, respectively.

However, there are two quantum paths with different emission times contributing to the emission peak from 1.5 o.c. to 2.0 o.c. for the combined field. The positive- and negative-sloped branches are corresponding to the short and long paths, respectively. Since the two paths have different emission times, it is difficult to obtain an isolated attosecond pulse through the superposition of harmonics. In fact, the laser intensity of the combined field near peak C″ is gradually augmented with increasing the peak intensity of the HCLF, which predicts that the electrons ionized near peak B′ will be accelerated to a longer distance. This will result in a lower recollision probability of the long path that the electrons travel for a longer time in the recombination process. Figure 4(a) shows the time-frequency distribution for the case of the combined field where the peak intensity of the fundamental field is $I_1 = 1\times10^{14}\,\mathrm{W/cm^2}$ and the peak intensity of the HCLF is $I_2 = 9\times10^{14}\,\mathrm{W/cm^2}$. We find that the long path of the emission peak almost from 1.5 o.c. to 2.0 o.c. is seriously suppressed. As only a single short quantum path contributes to the

HHG, the isolated attosecond pulse can be obtained directly by superposing several harmonics. Figures 4(b) and 4(c) show the time profiles of the attosecond pulses by superposing harmonics from the 320th to the 450th order for the HCLF with peak intensity $I_2 = 6 \times 10^{14}\,\mathrm{W/cm^2}$ and $I_2 = 9 \times 10^{14}\,\mathrm{W/cm^2}$, respectively. For the case of the HCLF with the peak intensity $I_2 = 6\times10^{14}\,\mathrm{W/cm^2}$, there are two attosecond pulses marked as 1 and 2, which are originated from the contribution of the short and long quantum paths as shown in Fig. 3(b), respectively. The intensity of pulse 2 is weaker than pulse 1. By increasing the peak intensity of HCLF to $I_2 = 9\times10^{14}\,\mathrm{W/cm^2}$, an isolated 75-as pulse is obtained as shown in Fig. 4(c). This result agrees well with that from the time-frequency distribution in Fig. 4(a), in which only a short quantum path contributes to the harmonic generation.

In summary, we have theoretically investigated the HHG from asymmetric molecular ions in the combined laser field, which is achieved by utilizing an HCLF to modify the fundamental driving laser field. Our results indicate evident advantages of using the combined field to manipulate the high-order harmonic generation. Based on the analysis of time-frequency distributions and electronic wave packet probability densities, the recombination channels are successfully simplified due to the fact that the electrons are mainly concentrated around the nucleus H^+. At the same time, by adding an HCLF with higher peak intensity to the fundamental laser field, the HHG cutoff is dramatically extended and a dominant short quantum path is easily selected to contribute to the high-order region in HHG. By superposing the proper range of the harmonics, an isolated 75-as pulse is directly obtained.

We sincerely thank Professor Han Keli and Dr. Lu Ruifeng for providing the LZH-DICP code.

References

[1] Brabec T and Krausz F 2000 *Rev. Mod. Phys.* **72** 545
[2] Wu Y and Yang X X 2007 *Phys. Rev.* A **76** 013832
[3] Wu Y and Yang X X 2007 *Phys. Rev. Lett.* **98** 013601
[4] Lein M 2005 *Phys. Rev. Lett.* **94** 053004
[5] Frolov M V, Manakov N L, Sarantseva T S, Sarantseva M Y, Ryabikin M Y and Starace A F 2009 *Phys. Rev. Lett.* **102** 243901
[6] Paulus G G, Lindner F, Walther H, Baltuke A, Goulielmakis E, Lezius M and Krausz F 2003 *Phys. Rev. Lett.* **91** 253004
[7] Esry B D and Ben-Itzhak I 2010 *Phys. Rev.* A **82** 043409
[8] Krausz F and Ivanov M 2009 *Rev. Mod. Phys.* **81** 163
[9] Corkum P B 1993 *Phys. Rev. Lett.* **71** 1994
[10] Goulielmakis E, Schultze M, Hofstetter M, Yakovlev V S, Gagnon J, Uiberacker M, Aquila A L, Gaullikson E M, Attwood D T, Kienberger R, Krausz F and Kleineberg U 2008 *Science* **320** 1614
[11] Xia C L and Liu X S 2013 *Phys. Rev.* A **87** 043406
[12] Feng X, Gilbertson S, Mashiko H, Wang H, Khan S D, Chini M, Wu Y, Zhao K and Chang Z 2009 *Phys. Rev. Lett.* **103** 183901
[13] Zeng Z N, Cheng Y, Song X H, Li R X and Xu Z Z 2007 *Phys. Rev. Lett.* **98** 203901
[14] Song X H, Zeng Z N, Fu Y X, Cai B, Li R X, Cheng Y and Xu Z Z 2007 *Phys. Rev.* A **76** 043830
[15] Zuo T, Chelkowski S and Bandrauk A D 1993 *Phys. Rev.* A **48** 3837
[16] Moreno P, Plaja L and Roso L 1997 *Phys. Rev.* A **55** R1593
[17] Zhu X, Zhang C J, Gu M L and Yao J P 2014 *Opt. Express* **22** 7947
[18] Bian X B and Bandrauk A D 2010 *Phys. Rev. Lett.* **105** 093903
[19] Miao X Y and Zhang C P 2014 *Phys. Rev.* A **89** 033410
[20] Miao X Y and Zhang C P 2014 *Laser Phys. Lett.* **11** 115301
[21] You D, Jones R R, Bucksbaum P H and Dykaar D R 1993 *Opt. Lett.* **18** 290
[22] Matos-Abiague A and Berakdar J 2003 *Phys. Rev.* A **68** 063411
[23] Yu C X, Liu S B and Song H Y 2013 *Phys. Rev.* A **87** 063407
[24] Pan Y, Zhao S F and Zhou X X 2013 *Phys. Rev.* A **87** 035805
[25] Zhang C J and Liu C P 2015 *New J. Phys.* **17** 023026
[26] Hu J, Han K L and He G Z 2005 *Phys. Rev. Lett.* **95** 123001
[27] Miao X Y and Du H N 2013 *Phys. Rev.* A **87** 053403
[28] He H X, Lu R F, Zhang P Y, Guo Y H, Han K L and He G Z 2011 *Phys. Rev.* A **84** 033418
[29] Lu R F, Zhang P Y and Han K L 2008 *Phys. Rev.* E **77** 066701
[30] Ben-Itzhak I, Gertner I, Heber O and Rosner B 1993 *Phys. Rev. Lett.* **71** 1347
[31] Liu K L, Hong W Y and Lu P X 2011 *Opt. Express* **19** 20279
[32] Burnett K, Reed V C, Cooper J and Knight P L 1992 *Phys. Rev.* A **45** 3347
[33] Lagmago Kamta G and Bandrauk A D 2005 *Phys. Rev. Lett.* **94** 203003